Alloying and oxidation of PdAu thin films

Thin Solid Films 790 (2024) 140212

Contents lists available at ScienceDirect

Thin Solid Films

journal homepage: www.elsevier.com/locate/tsf

Alloying and oxidation of PdAu thin films

Helen Edström [a,*], Andreas Schaefer [b], Leon Jacobse [c,d], Kim von Allmen [a], Benjamin Hagman [a], Per-Anders Carlsson [b], Johan Gustafson [a]

[a] Department of Synchrotron Radiation Research, Lund University, Box 118, 221 00, Lund, Sweden
[b] Department of Chemistry and Chemical Engineering, Chalmers University of Technology, Chalmersplatsen 4, 412 96, Gothenburg, Sweden
[c] Centre for X-ray and NanoScience CXNS, Deutsches Elektronen-Synchrotron DESY, Notkestraße 85, 226 07, Hamburg, Germany
[d] Department of Interface Science, Fritz Haber Institute of the Max Planck Society, Faradayweg 4-6, 141 95, Berlin, Germany

ARTICLE INFO

Keywords:
Alloying
Bimetallic system
Grazing-incidence X-ray diffraction
Oxidation
Oxide formation
Palladium–gold
Thin film

ABSTRACT

The relation between catalytic activity and the presence of oxides on the catalyst's surface has proven very complex, especially in the case of methane oxidation over Pd. While the metallic Pd surface and a thin, but at least two atomic layers thick, oxide film has been found catalytically active, a single-layer surface oxide or a too thick oxide film are both low-active. Unfortunately, under reaction conditions, the oxide tends to grow thick and deactivate. The reason for this deactivation is believed to be exposure of the PdO(100) surface, which does not have any suitable active sites for the methane adsorption and activation, in contrast to PdO(101), which is exposed for thin films. In an attempt to limit the thickness of the oxide film, and hence stabilise the active PdO orientation, we have investigated the oxidation of thin PdAu films. The effects of different mixtures (25%, 50%, and 75% Au, respectively) and treatments on the oxidation and orientation of the alloy and oxide films were investigated. As intended, PdAu turned out to be significantly more difficult to oxidise compared to pure Pd. This effect was even stronger than expected. Depending on the sample temperature and the amount of Au present in the alloy, the orientation of the oxide is affected. At lower temperatures and Au concentration, the desired [301] oxide orientation (corresponding to the (101) planes being parallel to the sample surface) is favoured, while higher Au concentration favours the low-active [100] oxide orientation. Thus, PdAu might be a good candidate for methane oxidation if the Au concentration is low, probably below 25%. The larger lattice constant of Au compared to Pd might also affect the oxide orientation, so another choice of alloying material, e.g. PdPt, may also work to stabilise PdO[301]. Independent of the alloy composition, the sample temperature during oxide growth should be optimised in order to achieve an active oxide film.

1. Introduction

Methane (CH_4) is a greenhouse gas that is about 30–80 times more potent than carbon dioxide (CO_2), depending on which timeframe is considered [1]. Hence, catalysts that are able to efficiently transform CH_4 to CO_2 and H_2O, for instance in the exhaust cleaning of gas-driven vehicles, are highly desired. The function of a catalyst is directly related to the surface configuration. As described by the so-called Sabatier principle [2], the catalytic surface needs to be reactive enough to activate the adsorbed reactants, but not too reactive, since this will result in large energy barriers for the creation and desorption of reaction products. This delicate dependency especially means that the formation of new phases on the surface, such as oxides, may completely change the catalytic properties of a material. Over the last decades, there has been a debate concerning the active phase of Pt-group metals for oxidation catalysis. In general, and especially for CO oxidation, the main conclusion is that the metallic surfaces are catalytically active, but often not stable under reaction conditions, while the activity of the oxides that may form during the reaction depends on the presence of coordinatively unsaturated (CUS) sites where the reactants can adsorb [3–5].

For methane oxidation, Pd is one of the best catalysts, but the relation between the presence of oxides and the catalytic activity has proven extra complicated. In a study of methane oxidation over a Pd(100) single crystal, Hellman et al. [3] found that the metallic surface is indeed active but unstable under reaction conditions. Furthermore, the initial oxide growth results in low activity but when the oxide becomes thicker, the activity increases up to a certain point, after which it decreases while the oxide continues to grow. The proposed hypothesis explaining this behaviour is illustrated in Fig. 1. Thin PdO films expose the (101) surface, with CUS Pd atoms in the surface, where

* Corresponding author.
E-mail address: helen.edstrom@sljus.lu.se (H. Edström).

https://doi.org/10.1016/j.tsf.2024.140212
Received 29 September 2023; Received in revised form 5 December 2023; Accepted 5 January 2024
Available online 8 January 2024

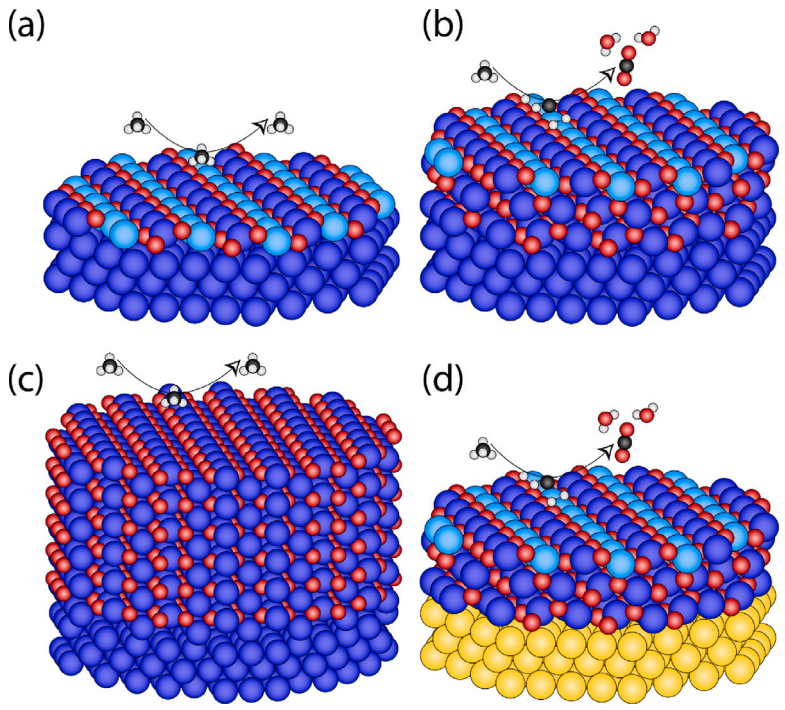

Fig. 1. CH_4 oxidation on different PdO structures on Pd(100). (a) One single layer of PdO is inactive for CH_4 oxidation. (b) A thin film of PdO (a few atomic layers) is active for CH_4 oxidation. (c) When the PdO film grows too thick, it becomes inactive. (d) By growing the PdO film on Au, the idea is to limit the thickness of the film to keep the catalytic activity. (Colours: off white – H, black – C, red – O, light blue – unsaturated Pd, dark blue – saturated Pd, yellow – Au).

the methane molecules are adsorbed and activated (Fig. 1b). When the oxide becomes thick enough, however, it is no longer coupled to the substrate and may expose the energetically favourable (100) surface [6], which lacks CUS sites and hence results in a low catalytic activity (Fig. 1c). The initial oxide consists of a single PdO(101) layer and exposes CUS Pd atoms (Fig. 1a), but has a different behaviour due to a ligand effect with the Pd layer below, as described by Martin et al. [4]. Hence, to create an active and stable methane oxidation catalyst, one would like to stabilise the thin, but at least two layers thick PdO film.

One idea proposed to achieve this goal is to limit the amount of Pd that can be oxidised with a bimetallic system with Pd and Au (Fig. 1d). Pd is more reactive than Au, so the reactants will pull out Pd atoms to the surface and may form a PdO film on top of the remaining Au. This proposal finds support in previous studies showing that PdAu often shows enhanced catalytic activity and selectivity, and also less self-poisoning [7]. Surprisingly little is known about the initial oxidation of PdAu thin films. Strømsheim et al. have, however, shown that a PdO surface oxide can be grown on $Pd_{75}Au_{25}$(100) at a pressure of 10^{-3} hPa [8], while Hilaire et al. have shown that Au rich PdAu alloys interact weakly with O [9]. Hence, this approach seems promising.

In this paper we report on an investigation of thin films of Pd and Au with 25%, 50%, or 75% Au content, grown on sapphire (0001) substrates, as a bimetallic system. Using grazing-incidence X-ray diffraction (GIXRD), we followed the mixing of Pd and Au into an alloy as well as the oxide formation in O_2 pressures up to about 500 hPa. Our main conclusions are that Au indeed hinders oxide formation, and this effect is surprisingly strong. For the most Au rich sample, not even 500 hPa O_2 was enough to create a detectable oxide at 670 K. Depending on the order of annealing and oxidation steps, we also found significant preferential ordering of the metal as well as the PdO films, relative to the substrate. This allows us to investigate the dominating orientations of the oxide films, which suggests that Pd rich films expose a rather even mixture of the desired [301] orientation (corresponds to the (101) planes being parallel to the sample surface) and low-active [100] orientations, while more Au favours [100]. We find that differences in lattice constant and/or sample temperature facilitates growth of differently oriented PdO films. Combined, our results suggest that the best PdAu mixture for methane oxidation is probably more Pd rich than what we have studied, since this will still limit the oxide growth significantly and at the same time expose more [101] oriented oxide. Further, preparing the oxide film at low temperature yields more of the desired orientation.

2. Materials and methods

The experiments were performed at the Swedish High-Energy X-ray Materials Science Beamline (P21.2) [10] at PETRA III, DESY, in Hamburg, Germany. The samples were placed in a high-vacuum chamber with a base pressure of 10^{-8} hPa, where exposure to gases was done through leak valves. At pressures above 10^{-3} hPa, the turbo pump was closed off, which allowed the pressure to be increased up to 1000 hPa in a batch mode. The samples were heated by a Boralectric heater and the sample temperature estimated by a calibration of temperature vs heating current performed at different gas pressures to account for the convection of heat.

The PdAu samples consisted of thin metallic films deposited on sapphire (0001) produced by Siegert Wafer. The samples can be divided into four main groups:

1. Pd_{20} — 20 nm pure Pd films as reference.
2. Pd_xAu_{20-x} — 20 nm films with Pd deposited before Au with Pd:Au ratios of 15:5, 10:10, and 5:15.
3. $Pd_{05}Au_{05}$ — 10 nm films with Pd deposited before Au with a Pd:Au ratio of 5:5.
4. $Au_{10}Pd_{10}$ — 20 nm films with Au deposited before Pd with a Pd:Au ratio of 10:10.

The samples were manufactured at the Nanofabrication laboratory MC2, Myfab Chalmers, in Gothenburg, Sweden, by electron-beam physical vapour deposition. A Lesker PVD 225 system was used for the deposition, at a pressure below $7 \cdot 10^{-7}$ hPa. The deposition thickness was determined using a quartz crystal microbalance sensor with predetermined material specific calibration data.

The GIXRD measurements were performed with an X-ray energy of 68 keV and a grazing incidence angle of 0.04°, just below the critical angle for total reflection for Pd, in order to maximise the surface sensitivity. The scattered X-rays were collected using a 2D detector (Varex Imaging XRD 4343CT) placed with the left edge about 2 cm to the right of the direct beam and with a sample-detector plane distance of 1.73 m, as calibrated from the Pd_{20} sample with pyFAI-calib2 [11]. A mask was used to block the diffraction from the beryllium cylinder of the vacuum chamber, limiting the Q range of the measurements to about 1.5–5.5 $Å^{-1}$. Furthermore, the detector was protected against the strong Bragg reflections of the sapphire substrate by tungsten pieces placed just in front of the detector.

For each measurement, the sample was rotated by 90° during continuous recording of 271 detector images. During the measurements, there were some slow variations in the diffraction intensities, showing that there is a weak preference for certain orientations of the metallic film relative to the substrate, with respect to rotation around the surface normal. In order to avoid any effect of this, all analysis was performed on the average of the detector images for each rotation.

The detector images were processed with Igor Pro 8 (WaveMetrics, Inc., Lake Oswego, Oregon) and HESXRD Analysis Toolkit (HAT) [12] and integrated using pyFAI-integrate [11]. Due to alignment difficulties (thermal drift), the total intensity and background varies significantly between measurements. To produce comparable data sets, a polynomial background was removed before normalising against the intensity of the peaks, weighted against the Pd:Au ratio to take the stronger scattering of Au into account.

3. Results

A first view of the data and how they were analysed is shown in Fig. 2, with the example of $Pd_{10}Au_{10}$ after oxidation at 670 K in 550 hPa O_2 for about 30 minutes. Fig. 2a shows a selected part of the averaged detector image from the measurement, where the sample is rotated around the surface normal. The main features are the powder diffraction rings showing that the film is crystalline but to a large extent randomly oriented.

In order to facilitate the identification of different phases, Fig. 2b shows an integrated diffractogram with intensity vs Q. This can be directly compared to the simulated diffractograms of metallic Pd and Au (c) as well as PdO (d). Hence, we can directly identify the presence of both metal (black dashed lines) and oxide (red dashed lines) in the diffraction pattern. The alloy peaks are found in the middle between the Pd and Au peaks, as expected for a 1:1 alloy according to Vegard's law, which is known to work well for PdAu [13]. For the rest of the paper, we limit the Q range of the diffractograms to 2.3–2.9 $Å^{-1}$ (the shaded area), which is enough to identify PdO, Pd, Au and PdAu alloy.

Returning to the 2D image in Fig. 2a, we find some extra bright reflections along the powder diffraction rings, marked by white and coloured rings for the metal and oxide, respectively. These reflections show that the film, although to a large extent randomly oriented, has a strong preference for specific orientations relative to the sample surface normal. In this case, the metal prefers a [111] orientation (solid white circles), while the oxide is mainly [100] oriented (green). To a lesser degree here, but stronger in other measurements below, we also see metal with [110] (dashed white), and PdO with [301] (pink) and [110] (yellow) orientations, where the [301] orientation corresponds to the PdO(101) planes being parallel to the sample surface. The vertical streaks extending from these reflections are crystal truncation rods (CTRs), which are always aligned perpendicular to a surface or interface. Thus, we can conclude that at least either the surface or one interface of the metal as well as the oxide, are parallel to the general sample surface.

By comparing the intensities of the oxide and metal signals within the shaded Q range, as well as the intensities of the peaks along the powder rings, we have very roughly estimated the degree of oxidation

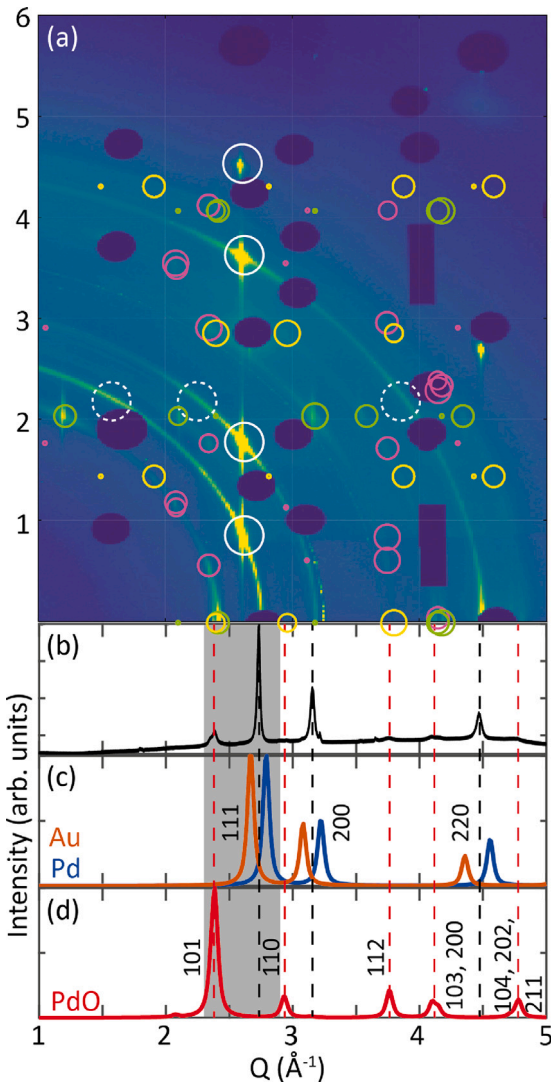

Fig. 2. Illustration of the data interpretation. GIXRD from a sample with 10 nm Pd and 10 nm Au on $Al_2O_3(0001)$ after oxidation in 550 hPa O_2 at 670 K. (a) A combined detector image corresponding to the average of all detector images during a 90° rotation around the surface normal. (b) Integrated diffractogram corresponding to (a). (c–d) Simulated diffractograms of Pd, Au and PdO, for comparison.

as well as the degree of preferential ordering into the above mentioned metal and oxide orientations. Note that the diffraction signals decrease with depth and the analysed part of the sample does not necessarily have the same Pd:Au ratio as the film in total. Instead it is typically enriched in Pd, as oxidation pulls Pd to the surface. A more thorough description of how this estimation was performed is found in Appendix. The results of this analysis are shown in Table 1.

3.1. Summary of results

Table 1 shows a summary of the different samples investigated. The treatments column shows each change of conditions leading up to the sample state, which was further analysed for degree of oxidation and preferential ordering. Between each change in conditions, we typically measured GIXRD, X-ray reflectivity (XRR), and GIXRD again, which took about 20 min. The quality of the XRR measurements was generally not very good and the results are omitted in this paper, but it helped us to confirm the film thickness of the samples. We are using the second GIXRD measurement for analysis. The first treatment row of each sample corresponds to vacuum conditions while the following

Table 1
Summary of results with rough estimates of degrees of oxidation and preferential ordering. For each sample investigated, column 2 describes, stepwise, the treatments leading to the oxidised state which was analysed further. The italic condition is when the metals were first mixed, the underlined is when the metal film started to become preferentially ordered, and the bold is when the first signs of oxidation was found. The following columns report a rough estimate of the degree of oxidation, degree of preferential order, how much of the preferentially ordered material that shows which orientation and whether the reflections show CTRs or not, for the metal and oxide. Due to the tetragonal unit cell of PdO, the [301] orientation corresponds to the PdO(101) planes being parallel to the sample surface.

Sample	Treatment	Oxidation	Metal			Oxide		
			Order	Orientation	CTRs	Order	Orientation	CTRs
Pd_{20}	RT - 770 K - RT 670 K - $1.2 \cdot 10^{-3}$ hPa - **1.5 hPa** - 45 min	26%	45%	[111] 92% [110] 8%	yes	16%	[100] 39% [110] 19% [301] 42%	yes
$Pd_{15}Au_{05}$	RT - 470 K - *620* K - 720 K - 770 K - RT 1 hPa - 420 K - 550 K - 670 K - **10 hPa** - 100 hPa - 400 hPa - 34 min - RT - vacuum	71%	95%	[111] 92% [110] 8%	yes	64%	[100] 35% [110] 14% [301] 51%	yes
$Pd_{10}Au_{10}$	RT - 470 K - *620* K - 720 K - 770 K - RT 1 hPa - 420 K - 550 K - 670 K - **10 hPa** - 110 hPa - 550 hPa - 28 min - RT - vacuum	18%	73%	[111] 88% [110] 12%	yes	44%	[100] 51% [110] 1% [301] 48%	yes
$Pd_{10}Au_{10}$	RT (no anneal in vacuum) 10 hPa - 420 K - *550* K - **670 K** - 100 hPa - 410 hPa - 35 min - RT	80%	30%	[111] 7% [110] 93%	no	2%	[100] 59% [110] 0% [301] 41%	no
$Pd_{10}Au_{10}$	RT (no anneal in vacuum) 490 hPa - 420 K - 860 hPa - *550* K - **620 K** - 670 K - 33 min - 620 K - 550 K - 420 K - RT - vacuum	36%	46%	[111] 0% [110] 100%	no	1%	[100] - [110] - [301] -	no
$Pd_{10}Au_{10}$	RT - 770 K - RT 470 hPa - 420 K - 550 K - 620 K, 550 hPa - **670** K - 36 min - 620 K - 550 K - 420 K - RT - vacuum	53%	66%	[111] 89% [110] 11%	yes	7%	[100] 23% [110] 11% [301] 66%	yes
$Pd_{05}Au_{15}$	RT - 470 K - *620* K - 720 K - RT 1 hPa - 420 K - 550 K - 670 K - 10 hPa - 100 hPa - 410 hPa - 40 min - RT	3%	71%	[111] 100% [110] 0%	yes	–	[100] - [110] - [301] -	–
$Pd_{05}Au_{05}$	RT - 470 K - *620* K - 720 K - 770 K - RT 1.3 hPa - 670 K - 11 hPa - **100 hPa** - 490 hPa - 28 min - RT	32%	81%	[111] 92% [110] 8%	yes	34%	[100] 64% [110] 9% [301] 27%	yes
$Au_{10}Pd_{10}$	RT - 470 K - *620* K - 720 K - 770 K 670 K - **100 hPa** - 410 hPa - 17 min - RT	70%	76%	[111] 100% [110] 0%	yes	62%	[100] 60% [110] 1% [301] 38%	yes
$Au_{10}Pd_{10}$	RT (no anneal in vacuum) 1000 Pa - 420 K - ***550* K** - 670 K - 100 hPa - 400 hPa - 21 min - RT	86%	56%	[111] 100% [110] 0%	yes	19%	[100] 0% [110] 2% [301] 98%	no

rows correspond to exposure to O_2. Within the treatments, significant changes are indicated as special typesetting as follows; italic = PdAu are properly mixed; underlined = the metal shows preferential ordering; bold = first signs of oxidation.

As an example, the $Pd_{15}Au_{05}$ sample was initially annealed stepwise in vacuum, during which the metal mixed at 620 K and started to show preferential order at 770 K. After heating to 670 K and increasing the O_2 pressure to 10 hPa, we saw the first signs of an oxide. After oxidation in 400 hPa O_2 at 670 K followed by cooling down to room temperature, the metal film was oxidised to 71%, the metal was preferentially ordered to 95%, of which 92% was [111] oriented and 8% was [110] oriented, and the oxide was ordered to 64% with a mixture of different orientations.

3.2. Pure Pd

As reference, Fig. 3 shows the diffractograms and GIXRD images recorded for Pd_{20}, while varying temperature and O_2 pressure. The pristine sample shows a broad Pd peak at room temperature and vacuum, indicating that the Pd film is rather disordered. This is also indicated by the broad powder diffraction rings in Fig. 3b. Annealing the sample at 770 K in vacuum for 10 min and letting it cool to room temperature results in a significant increase of the ordering, indicated by a narrower peak in the diffractogram and by sharper powder rings and strong reflections in Fig. 3c.

For the oxidation, we first heated the sample to 670 K and dosed $1.2 \cdot 10^{-3}$ hPa O_2. This is expected to at least result in a Pd surface oxide, as found by Lundgren et al. after exposing Pd(111) single crystals to $5 \cdot 10^{-6}$ hPa O_2 at 570 K for 600 s [14]. Since the present GIXRD measurements are not sensitive to single layers, however, we cannot confirm this. After increasing the O_2 pressure to 1.5 hPa, the oxide signal started to appear very slowly (Fig. 3d). Keeping the sample under these conditions for 45 min resulted in further oxidation and increased preferential order, as shown by the sharper peak in the diffractogram and the more intense rings with sharp reflections in the detector image (Fig. 3e).

3.3. Alloying of $Pd_{10}Au_{10}$

Turning to the alloy samples, Fig. 4 shows the diffractograms for $Pd_{10}Au_{10}$ when heated stepwise in vacuum. The measurement of the pristine sample shows broad peaks at $Q = 2.666$ Å^{-1} and $Q = 2.772$ Å^{-1} corresponding to poorly ordered 111 reflections of Au and Pd, respectively. The Au peak is significantly stronger, as expected since the Au is deposited on top of the Pd and the X-ray scattering intensity scales with Z^2. At 470 K, the two peaks have moved slightly closer together and at 620 K, they have merged into a single peak, showing that the metals have mixed into an alloy. As the temperature is increased further to 720 K and 770 K, the peak continues to get sharper.

In the final measurement of Fig. 4, the sample is cooled down to room temperature. Due to problems with alignment during heating and cooling, the measurement performed at room temperature in vacuum failed. Hence, we show the measurement done after exposing to 1 hPa of O_2 instead. At this temperature, however, we do not expect any oxidation to take place, and we consider this measurement to be representative of the alloyed sample in vacuum. Cooling the sample results in a shift of the metal peak to 2.714 Å^{-1} which, according to

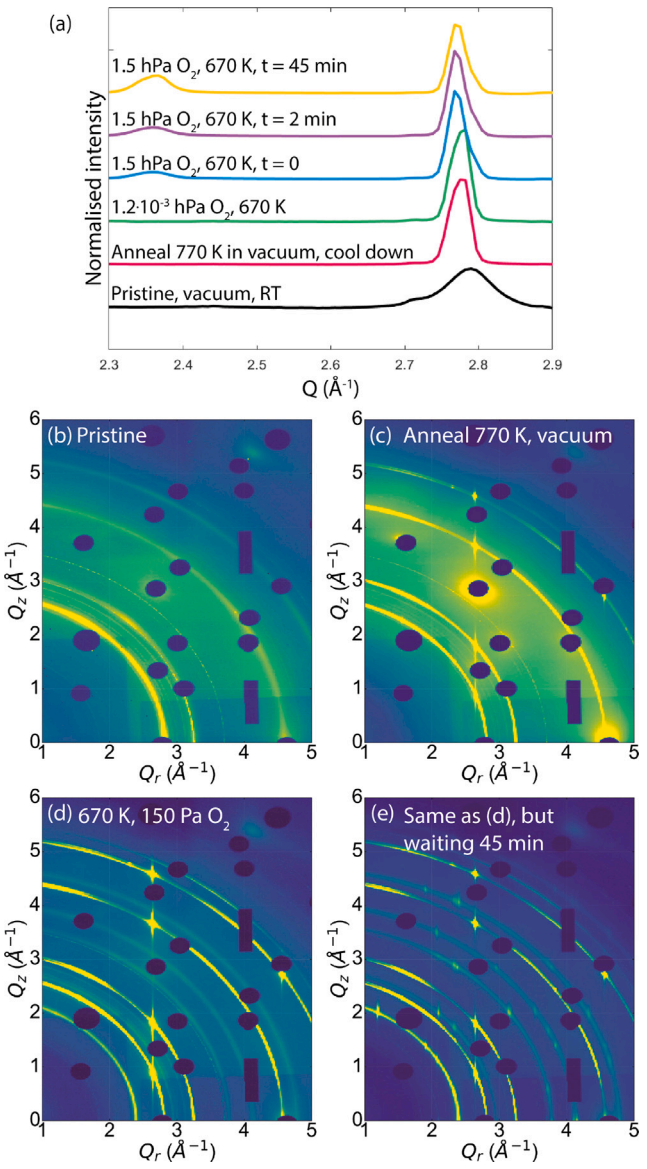

Fig. 3. Surface ordering and oxide formation on Pd_{20}. (a) The pristine sample was annealed at 770 K in vacuum and then cooled down to room temperature. After that, the sample was exposed to first $1.2 \cdot 10^{-3}$ hPa and then 1.5 hPa O_2 at 670 K. While no oxide signal could be detected at the lower pressure, it slowly developed at the higher, being clearly visible after 45 min. (b)–(e) GIXRD images corresponding to some of the diffractograms in (a), showing the ordering of the Pd film by annealing and the slow oxide growth in 1.5 hPa O_2 at 670 K.

Vegard's law, corresponds to a Pd:Au ratio of about 45:55, close to the expected 50:50.

The alloying is also shown in the detector images in Fig. 4b–d. For the pristine sample the Pd and Au rings are clearly separated but they merge into one at 620 K. At this point, the crystallites are still mainly randomly oriented, as shown by the lack of stronger reflections along the powder diffraction rings. Heating further to 770 K, we see that the crystallites order preferentially in the [111] orientation, as discussed above.

3.4. Oxidation of $Pd_{10}Au_{10}$

The alloyed $Pd_{10}Au_{10}$ sample was then heated in 1 hPa O_2 up to 670 K followed by a further stepwise increase of the O_2 pressure to 550 hPa, see Fig. 5. In the zoomed-in plot to the left, we can see a very weak oxide signal at 10 hPa, but only at the highest pressure investigated, it develops into a clear peak. This grows even further during cooling down to room temperature, suggesting that the optimal temperature for oxide growth is somewhat lower than 670 K.

3.5. Different mixtures of Pd and Au

Fig. 6 shows the diffraction after oxidation at 670 K of samples with different Pd:Au ratios. The shown measurements were done after a 45 min exposure to 1.5 hPa O_2 for the pure Pd sample, while the other three samples were exposed to around 500 hPa for 1–2 h. Although one should be very careful when comparing these measurements, we can find that these treatments result in fairly low degrees of oxidation for Pd_{20} and $Pd_{10}Au_{10}$, while the oxide on $Pd_{15}Au_{05}$ sample is significantly thicker. Furthermore, the first signs of oxidation (not shown here) were found at an O_2 pressures of about 1 hPa for Pd_{20}, while $Pd_{15}Au_{05}$ and $Pd_{10}Au_{10}$ required 10 hPa O_2 to start forming oxide. $Pd_{05}Au_{15}$ did not show any oxidation even at the highest pressure. Comparing the detector image in Fig. 6e to those in Fig. 6b–d, it can be seen that the oxide rings are missing for $Pd_{05}Au_{15}$.

3.6. Thinner film

$Pd_{05}Au_{05}$ and $Pd_{10}Au_{10}$ have the same relative Pd:Au ratios, but their metal layer thicknesses are different. Fig. 7a shows the peaks for oxidised $Pd_{05}Au_{05}$ and $Pd_{10}Au_{10}$. The most notable observation is probably that the metal peak is significantly more intense for $Pd_{10}Au_{10}$ compared to $Pd_{05}Au_{05}$, though they have been exposed to roughly the same amount of O_2 for approximately the same time. Looking at the GIXRD images in Fig. 7b–c provides us with a clue to the difference in metal peaks. Comparing $Pd_{05}Au_{05}$ to $Pd_{10}Au_{10}$ in Table 1, it can be seen that the degree of ordering is quite similar for both the metal phase and the oxide phase, but the degree of oxidation differs. $Pd_{05}Au_{05}$ has almost twice the degree of oxidation as $Pd_{10}Au_{10}$. Since there is half as much metal on the former sample, the absolute amount of formed PdO then might be the same as for the latter sample. While the most common orientation for the metal was [111] for both samples, there was more difference regarding the orientation of the oxide. The [100] orientation was highly dominating on $Pd_{10}Au_{10}$, but on $Pd_{05}Au_{05}$, [101] was the most common orientation (though less predominant). This is most likely due to a small difference in treatment, rather than film thickness, as discussed further below.

At the start of the oxidation process, the pressure was increased to about 1 hPa at room temperature, followed by heating to 670 K. For $Pd_{05}Au_{05}$, the heating was done in one step, while for $Pd_{10}Au_{10}$ it was done stepwise. Hence the oxide seeds, although not visible in the diffraction, might form at different temperatures and show different behaviour.

3.7. Different treatments

Fig. 8 compares the oxidation of $Pd_{10}Au_{10}$ with and without annealing in vacuum and when the sample is heated before or after the O_2 pressure is increased to the pressure where the oxide is found. The most obvious difference is in the preferential ordering depending on if the sample was annealed prior to oxidation or not. As found above, the preferential ordering of the metal layer occurs when annealing at 770 K, while 720 K is not enough. As the oxidation is done at 620–670 K, this is not enough to create a well-ordered surface. Not surprising, an ordered metal film is a requirement for an ordered oxide. There is, however, a significant difference between the annealed samples depending on whether the temperature or O_2 pressure was set first during the oxygen treatment. Setting the temperature first (Fig. 8b) gives strong preferential order in both the metal and the oxide, while setting the pressure first (Fig. 8c) gives significantly less order of the oxide. This might be because the oxidation process starts at a lower

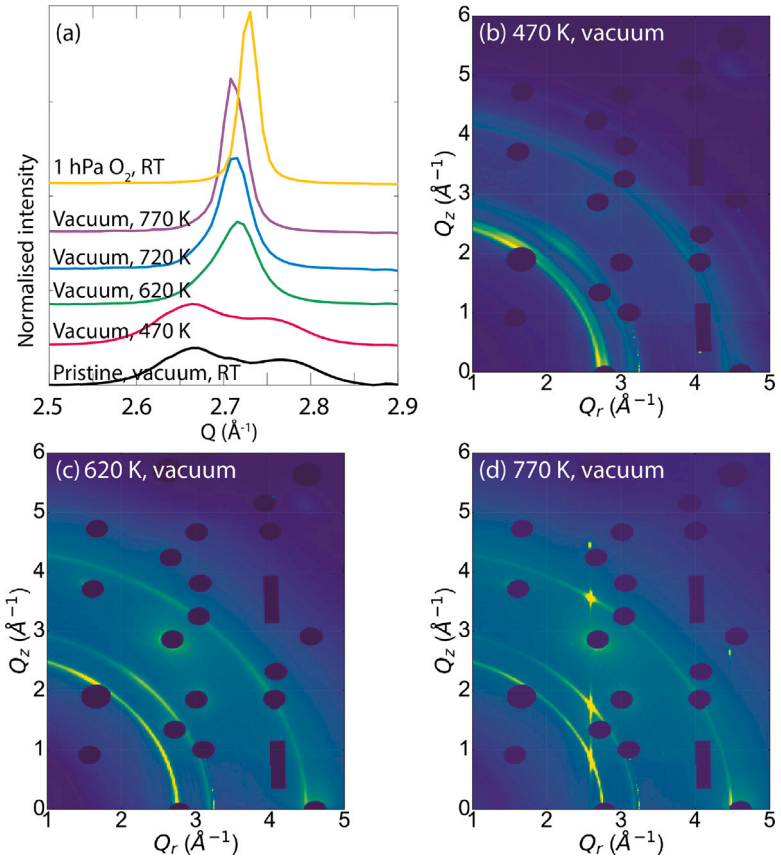

Fig. 4. Alloy formation in $Pd_{10}Au_{10}$. (a) For the pristine sample, we see a broad feature including a larger Au peak with a smaller Pd shoulder on the right side. When heated to 470 K (b), the Pd peak becomes much larger. Further heating to 620 K (c) gives a single peak with a position between the Au peak and the Pd peak; the sample is alloyed. Even further heating (d) makes the peak sharper, i.e. the alloy becomes more ordered. Cooling down to room temperature makes the peak shift to higher Q value due to temperature driven lattice compression.

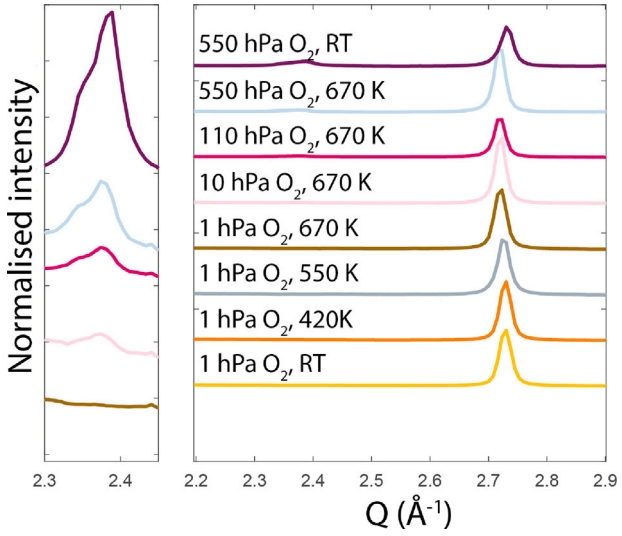

Fig. 5. Oxide formation on $Pd_{10}Au_{10}$. The oxidation is very slow until the O_2 pressure is increased to 550 hPa. Zooming in on the oxide peak, however, we find that the first signs of oxide appears at 10 hPa.

temperature, resulting in randomly oriented seeds that do not line up later on in the growth process.

Although the preferential ordering is significantly less pronounced in the samples that were not annealed, there are still stronger reflections along the powder rings. Interestingly, these reveal a Pd[110] orientation rather than Pd[111] as found above. For the oxide, only the sample which was annealed and when the temperature was set first shows significant preferential ordering (44% compared to only a few percent for the other $Pd_{10}Au_{10}$ samples), with approximately half of the oxide displaying the PdO[100] orientation and the other half displaying the PdO[301] orientation (51% and 48%, respectively).

Annealing also seems to make it more difficult to oxidise the sample. The reason for this is probably that oxygen more easily penetrates a less well-ordered surface. With these results in mind, it is a bit surprising that the sample where the oxygen pressure was increased before the temperature (panel e) is less oxidised than the one where the temperature was set first (panel d). The most likely reason for this is probably that the oxidation, by mistake, took place at 620 K instead of 670 K, which reduces the mobility and hence the grade of oxidation.

Another difference in treatment, which we at first neglected, also seems to affect the ratio between [100] and [301] oriented PdO. Comparing the first $Pd_{10}Au_{10}$ sample with $Pd_{05}Au_{05}$, we would expect them to behave similarly, due to the similar Pd:Au ratio. As mentioned above, the heating of $Pd_{05}Au_{05}$ was done in one step while the heating of $Pd_{10}Au_{10}$ was done stepwise. This may explain why there is a significantly stronger preference for PdO[100] in the $Pd_{05}Au_{05}$ sample.

A similar preference is found for the annealed $Au_{10}Pd_{10}$ (Pd on top) sample, which after the anneal also would be expected to behave similarly. For this sample, the temperature was set to 670 K before dosing any oxygen, and as for the $Pd_{05}Au_{05}$ sample, the oxidation started at the high temperature.

3.8. Pd on top

Finally, we studied two samples where Au was deposited before Pd. As we are interested in growing Pd oxide films, this would seem

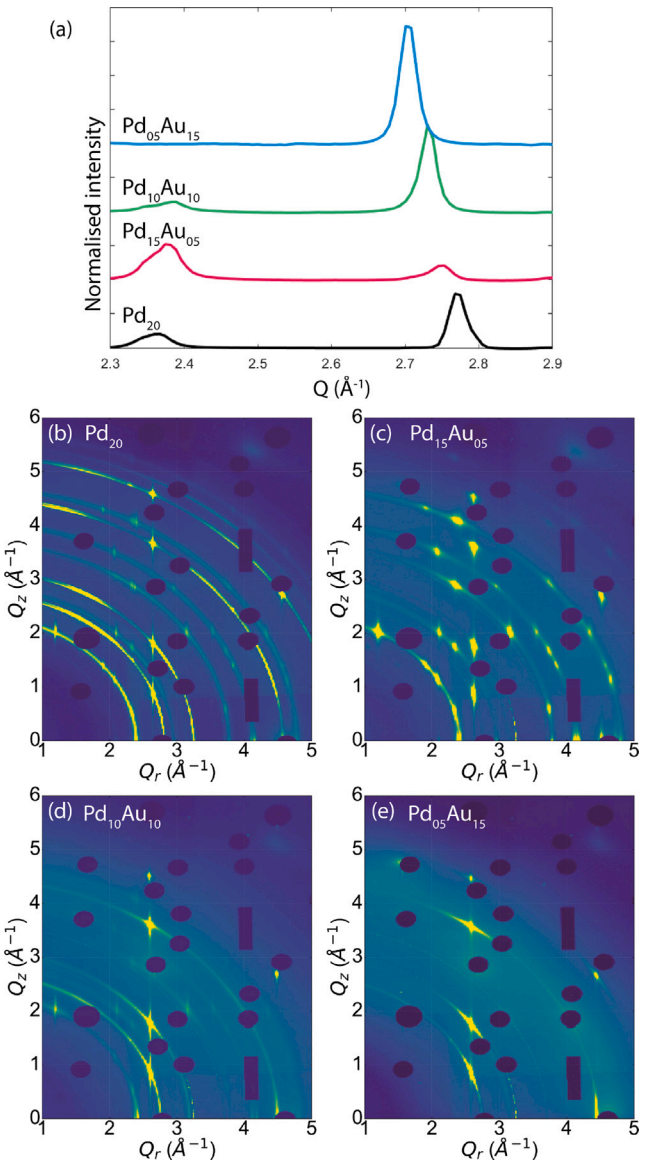

Fig. 6. Surface ordering and oxide formation on thin films with different mixtures of Pd and Au. (a) Diffractograms displaying metal and oxide peaks for different Pd:Au ratios. On Pd_{20} (b), the oxide formed at 1.5 hPa O_2 at 670 K and this measurement was recorded after 45 min under these conditions. For $Pd_{15}Au_{05}$ (c) and $Pd_{10}Au_{10}$ (d) the oxide signal started to appear at 10 hPa, but only after increasing the pressure to about 500 hPa, the oxide growth was significant. Both these samples were exposed to the highest pressure and temperature for almost 1.5 h. $Pd_{05}Au_{15}$ (e) did not show any signs of oxide formation, even after 1.5 h in 410 hPa O_2 at 670 K.

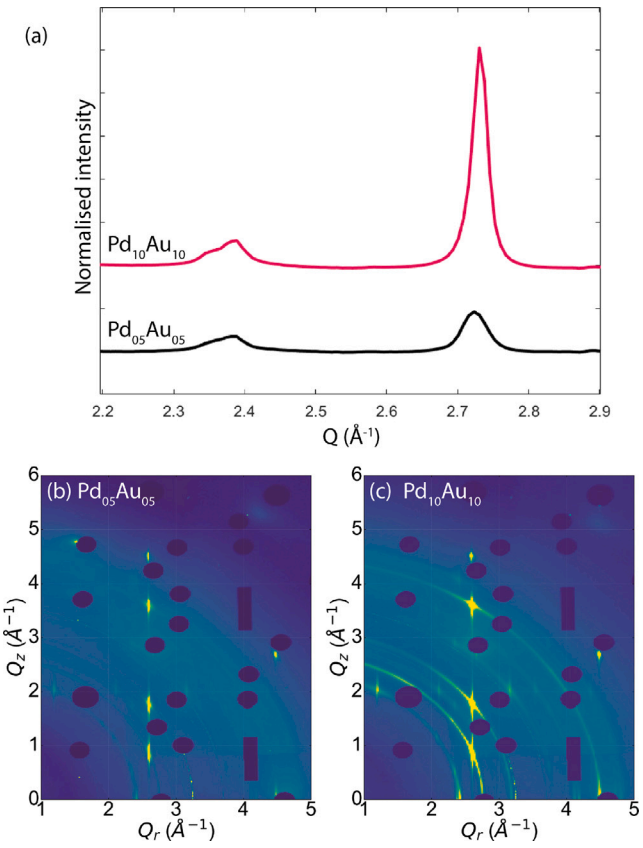

Fig. 7. Surface ordering and oxide formation on films with different thickness. (a) The significantly more intense metal peak for $Pd_{10}Au_{10}$ is caused by the contribution from the brighter ring compared to $Pd_{05}Au_{05}$. (b) The $Pd_{05}Au_{05}$ has been oxidised for 28 min. (c) The $Pd_{10}Au_{10}$ sample has also been oxidised for 28 min.

a natural approach. However, the main reason for not doing this is that Au does not wet the sapphire substrate very well [15]. In addition, we are interested in limiting the PdO thickness, which might be more effective with Au on top. The initial annealing step (when included) is also expected to mix the metals, rendering the deposition order irrelevant.

Fig. 9 shows a comparison between $Pd_{10}Au_{10}$ and $Au_{10}Pd_{10}$, with and without annealing. As expected, the annealed samples (panels b and c) are very similar. The reflections are a bit fuzzier and the CTRs much weaker for $Au_{10}Pd_{10}$, which is probably related to the low degree of wetting. For the samples that are not annealed (panels d and e), there is a more significant difference. As expected, when the metals are not mixed, $Au_{10}Pd_{10}$ is more easily oxidised than $Pd_{10}Au_{10}$. Furthermore, especially the metal becomes preferentially ordered, in the [111] orientation, when Pd is deposited on top (Fig. 9e). As the oxidation process takes place at the surface, without any diffusion of Pd through the Au layer, the metal underneath seems to be able to rearrange and line up with the sapphire substrate. The PdO film is also preferentially ordered, although to a lower degree, and interestingly, the orientation seems to match the desired PdO[301] rather than [100] for this sample.

4. Discussion

We have investigated a set of bimetallic films with Pd and Au grown on sapphire substrates, in order to follow their alloying and oxidation behaviours depending on mixture and different treatments.

When annealing in vacuum, we found that the metals were separated in the pristine sample and started to mix between 470 K and 620 K. This is in good agreement with a study of PdAu surface alloys on Pd(111) by Li et al. [16], showing that Au grows on Pd(111) in a Frank–van der Merwe growth mode at room temperature, and annealing at 600 K causes the Au atoms to diffuse into the bulk. In another study, of 6 nm PdAu bimetallic colloidal particles [17], Lee et al. suggested that a temperature of at least 400 K is needed to have significant atomic intermixing of Pd and Au, and at ~570 K, the intermixing is complete and the system has gone from bimetallic to alloy. Interestingly, we find an extra step of preferential ordering with the substrate upon further annealing to 770 K.

As expected, the alloy samples were more difficult to oxidise than a pure Pd film. For the first signs of oxidation in the diffraction signal to appear, the pure Pd sample was exposed to about 1 hPa O_2, while the alloy films with 25% and 50% Au required an O_2 pressure one order of magnitude higher. The film with 75% Au did not oxidise even at

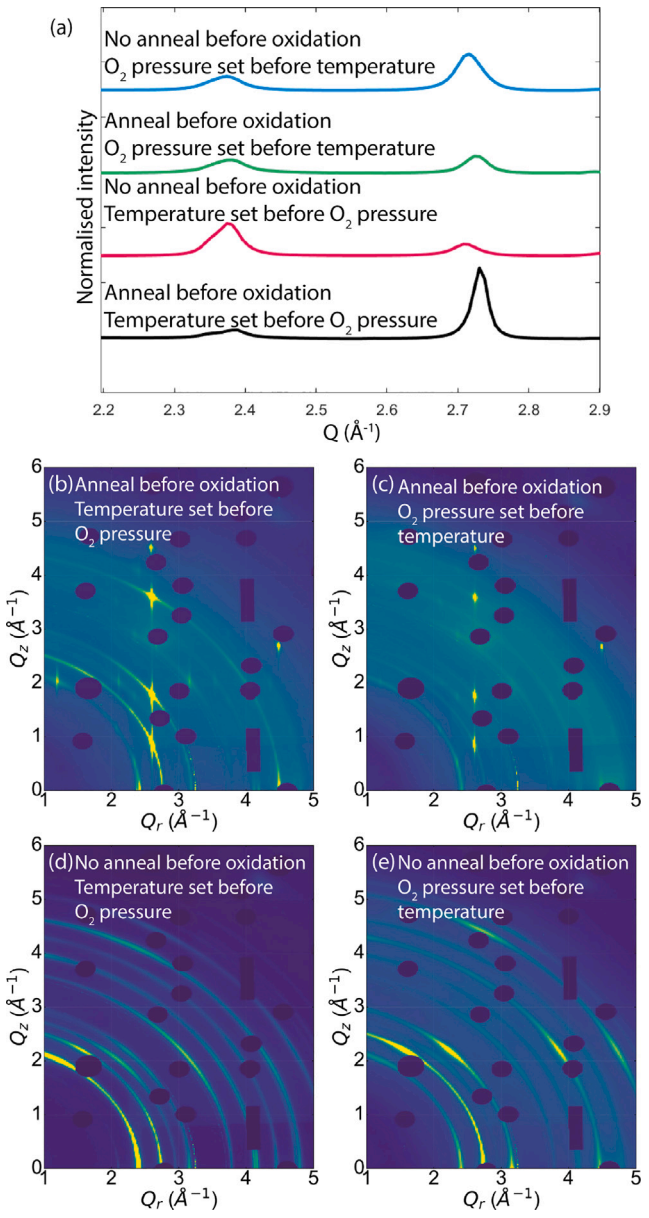

Fig. 8. Oxide formation on $Pd_{10}Au_{10}$ undergoing different treatments. (a) Diffractograms displaying metal and oxide peaks for different treatments. In (b) and (c), the sample was annealed to 770 K in vacuum before oxidation, in (b) and (d), the oxidation temperature was set before increasing the pressure and in (c) and (e), the pressure was set before increasing the temperature. Annealing is necessary for a well-ordered metal film with CTRs, which is in turn important for a well-ordered oxide film. Increasing the temperature before the O_2 pressure gives better order of the oxide. The sample that was not annealed and was exposed to O_2 before heating (e), however, shows a clear preferential ordering of the metal in the [110] orientation, in contrast to the more usual [111].

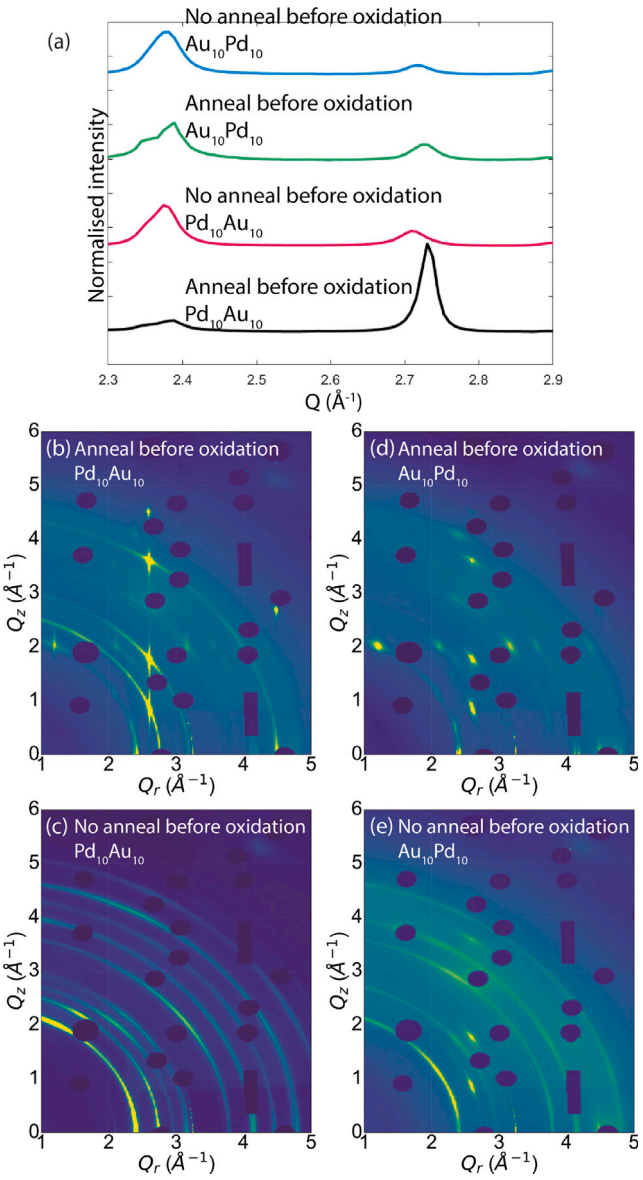

Fig. 9. Surface ordering and oxide formation on $Pd_{10}Au_{10}$ and $Au_{10}Pd_{10}$. (a) In all these cases, the temperature was increased prior to the O_2 pressure. (b) Annealed $Pd_{10}Au_{10}$ was oxidised at 670 K and 110 hPa O_2. (c) Annealed $Au_{10}Pd_{10}$ was oxidised at 670 K and 100 hPa O_2. (d) $Pd_{10}Au_{10}$ that was not annealed was oxidised at 670 K and 10 hPa O_2. (e) $Au_{10}Pd_{10}$ that was not annealed was oxidised at 550 K and 10 hPa O_2.

the highest O_2 pressure investigated, i.e. ~500 hPa. Considering the results by Strømsheim et al. [8], showing that a surface oxide grows on $Pd_3Au(100)$ already at 10^{-3} hPa O_2 and 570 K, however, we find the increase in oxidation resistance surprisingly strong.

On the other hand, Hilaire et al. [9] investigated PdAu alloys with varying concentrations using Auger electron spectroscopy and X-ray photoelectron spectroscopy and found that alloys with an Au content of more than 85% interact very weakly with O at temperatures below 870 K, while more Pd rich alloys start reacting with O at 570 K and get a Pd enriched surface. This is in agreement with the lack of oxidation of our most Au rich sample. At temperatures above 870 K, PdO decomposes, and hence it is expected that the Au rich samples are very inert to oxidation.

Not surprisingly, the history of the sample affects the structure of the oxidised sample. In order to have a well-ordered metal film underneath the oxide, the sample needs to be annealed before oxidation. Naturally, if the metal is not ordered, nor will the oxide on top be. The ordering of the oxide is, however, also depending on the order in which the conditions for the oxidation are set. If the temperature is set before dosing O_2, the oxide becomes better ordered than if the oxygen pressure is set before heating. In the latter case, the oxidation starts as soon as the temperature, and hence the atom mobility, is high enough to allow for mixing. This will, however, not be enough to create a well-ordered oxide structure, and the initial oxide seeds will be rather randomly oriented. Once these seeds have grown large enough, they will not easily rearrange to a preferential order.

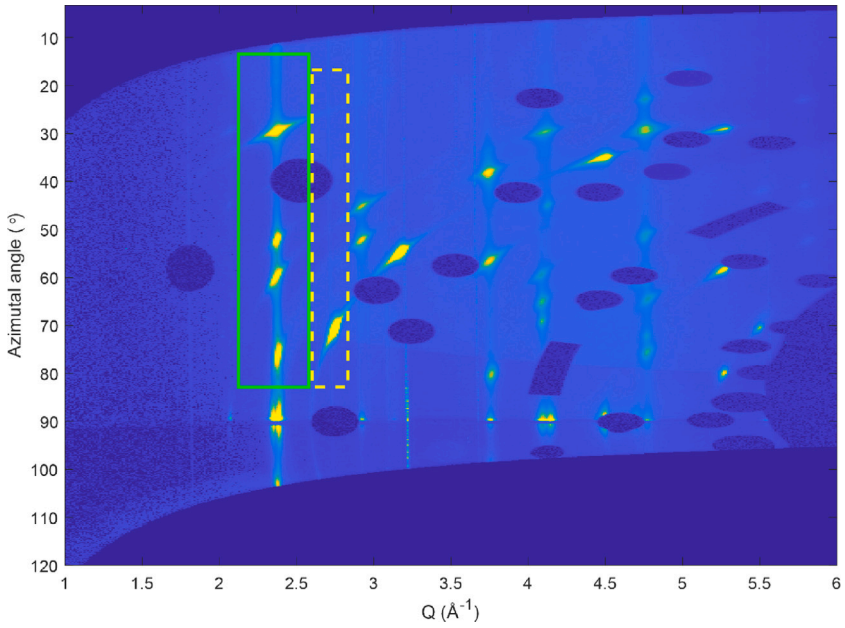

Fig. 10. Azimuthal integration of the $Pd_{15}Au_{05}$ diffraction pattern for analysis of degree of oxidation and preferential ordering. The intensity is shown as a function of Q and azimuthal angle relative to the vertical scattering direction. The green solid and yellow dashed boxes show the areas used for the analysis of the oxide and metal, respectively.

It is, however, not only the degree of order that varies between the different treatments, but also the orientation. While the metal prefers to order in a [111] orientation when annealed in vacuum, the sample exposed to O_2 at room temperature (without annealing) and then heated, shows preferential ordering in the [110] orientation. This is also something we have noticed during CO oxidation in experiments that are too incomplete to include here. This behaviour is, however, reversed when the deposition order is changed such that the Pd is grown on top of the Au. In this case, the metal orders in the [111] orientation and the oxidation happens at a significantly lower temperature. As the oxidation does not require any rearrangement of the bulk of the metal film, in order to pull Pd to the surface, the metal underneath is free to order in a similar way as when annealed in vacuum, while the oxidation proceeds in the surface region.

When investigating the orientation of the oxide, we discovered signals from PdO[301], PdO[110], and PdO[100], where the [301] orientation corresponds to PdO(101) planes being parallel to the sample surface. Comparing the second and third sample in Table 1, suggests that there is a slight preference for PdO[100] in the $Pd_{10}Au_{10}$ sample, while the more Pd rich $Pd_{15}Au_{05}$ favours PdO[301].

On Pd(100), there is a good match between the PdO(101) planes and the Pd surface lattice, and hence a strong preference for PdO growth with [101] orientation [18]. The preferential [111] ordering of the metal found here, however, makes comparison with Pd(111) more relevant. Here, it is not possible to find a very good match between any PdO orientation and the metal surface, but for PdO(100), the match becomes better if the metal lattice is expanded, as when alloyed with Au. This can explain the change in preference related to the mixing ratio.

Kan and Weaver report that, on Pd(111), as on Pd(101), PdO grows in the [301] orientation [19]. Kasper et al. on the other hand, found a mixture of [301] and [100] oriented PdO [20]. The main differences between these studies are that Kan and Weaver used atomic oxygen and sample temperature of 500K, while Kasper et al. used molecular oxygen and 670 K. In a very recent study by Mehar et al. [18], it is found that, also on Pd(100), it is possible to grow a mixture of [101] and [100] oriented PdO, and that the sample temperature plays a crucial role in determining the mixture. At low temperatures, [101] oriented PdO seeds are meta-stable and facilitate the corresponding growth. At high temperatures, however, the seeds are unstable and hence the growth is more random, resulting in both [101] and [100] oriented PdO. The breaking point is found around 600 K.

Returning to the present study, the oxidation occurred at about 670 K, well within the high temperature regime. Hence, it is likely that the sample temperature promotes a mixed orientation. Especially, while most of the samples were heated stepwise in oxygen (although in too low O_2 pressures to grow detectable oxides), the $Pd_{05}Au_{05}$ sample was heated directly to 670 K in O_2 and for the annealed $Au_{10}Pd_{10}$ sample, the temperature was set to 670 before any O_2 exposure. These two samples, by far, show the largest amount of [100] oriented PdO. Hence, we interpret the large amount of [100] oriented PdO as being a result of the high oxidation temperature, necessary to oxidise the alloy, and the larger lattice of Au (and the alloy) as compared to pure Pd.

In order to maximise the PdO[101] orientation, we propose to (i) attempt more careful oxidation at lower temperatures, (ii) use PdAu samples with lower Au concentrations, probably lower than 25%, and (iii) change the Au to something that is close to Pd in lattice constant, such as Pt. For the latter suggestion, theoretical calculations by Løvvik et al. indicate that when Pt and Pd are alloyed, Pt has positive segregation energy, meaning it will segregate deeper down into the bulk and leave Pd on the surface, while Au has negative segregation energy and will segregate towards the surface [21].

5. Conclusions

Thin films of Pd and Au on a substrate of Al_2O_3(0001) have undergone annealing and oxidation treatments and been investigated with GIXRD. Previous studies have indicated that thin PdO films, on pure Pd, expose the catalytically active (101), while thicker oxide films instead expose the low-active (100) surface. The aim of this study was to add Au in order to limit the oxidation and stabilise the PdO[301] orientation.

As the main result, we find that PdAu is indeed significantly more difficult to oxidise than pure Pd, more so than we expected. In order to significantly oxidise the alloys with 25% and 50% Au, within a timeframe of about an hour, an O_2 pressure of about 500 hPa was needed. For the sample with 75% Au, not even this resulted in any signs of oxidation.

Apart from the differences between samples of varying Pd:Au ratios, the order in which the samples were exposed to gas and heat affected the oxidation and, especially, the ordering of the metal and oxide films.

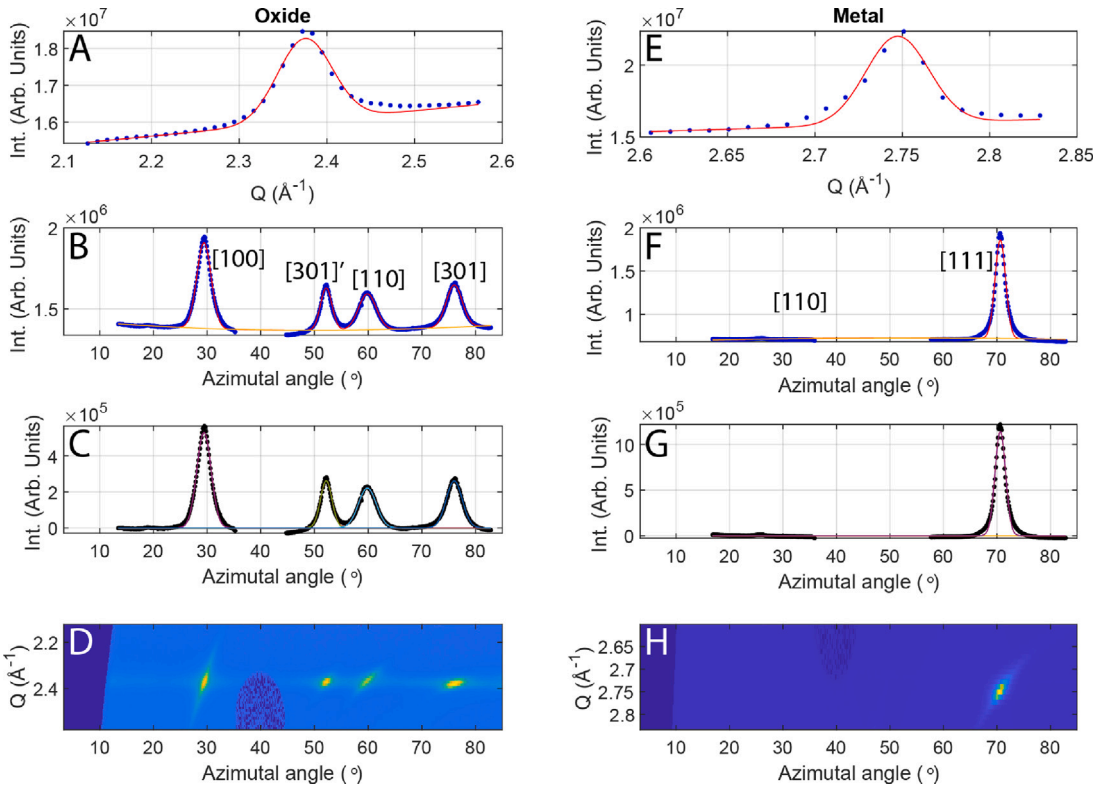

Fig. 11. Analysis of degree of oxidation and preferential ordering of oxide (A–D) and metal (E–H), respectively. D and H, the parts of the azimuthal integration, shown in Fig. 10, which are used for the analysis. A and E, projection of intensity on the *Q* axis, with a fit extracting the total intensities of the oxide and metal respectively. B and F, projection of intensity azimuthal angle axis, together with the fitted background in yellow and the total fit in red. C and G, the same data with background subtracted, together with the Gaussians fitted to the different peaks.

Most significantly, the metal underwent preferential ordering, typically in the [111] orientation, upon annealing in vacuum at about 770 K, while the oxide was preferentially ordered if the sample was annealed and the temperature was increased prior to dosing O_2. The orientation of the oxide turned out to be a mixture of, mainly, [100] and [301], with the amount of the desired [301] orientation increasing with decreasing Au content and lower oxidation temperature. The temperature effect is likely related to the stability of [301] oriented PdO seeds, while the Pd:Au ratio affects the matching in the metal-oxide interface.

Based on the above conclusions, we believe that oxide growth at lower temperatures, combined with an even lower Au content than 25%, might give the desired result. The degree of oxidation will still be limited and the amount of PdO[301] will increase. Alternatively, replacing Au with Pt is also expected to hinder oxide growth, but with a very small change of lattice constant as compared to pure Pd.

CRediT authorship contribution statement

Helen Edström: Conceptualization, Data curation, Formal analysis, Investigation, Methodology, Validation, Visualization, Writing – original draft, Writing – review & editing. **Andreas Schaefer:** Conceptualization, Data curation, Formal analysis, Investigation, Methodology, Validation, Visualization. **Leon Jacobse:** Data curation, Formal analysis, Investigation, Validation, Visualization. **Kim von Allmen:** Investigation. **Benjamin Hagman:** Investigation. **Per-Anders Carlsson:** Investigation, Methodology. **Johan Gustafson:** Conceptualization, Data curation, Formal analysis, Funding acquisition, Investigation, Methodology, Project administration, Supervision, Validation, Visualization, Writing – original draft, Writing – review & editing.

Declaration of competing interest

The authors declare that they have no known competing financial interests or personal relationships that could have appeared to influence the work reported in this paper.

Data availability

Data will be made available on request.

Acknowledgements

We acknowledge DESY (Hamburg, Germany), a member of the Helmholtz Association HGF, for the provision of experimental facilities. Parts of this research were carried out at PETRA III and we would like to thank Ulrich Lienert, Zoltán Hegedűs, Malte Blankenburg, and Sven Gutschmidt for assistance in using the Swedish High-Energy X-ray Materials Science Beamline. Beamtime was allocated for proposal 11011929. We would also like to thank John Andersson, at the Department of Chemistry and Chemical Engineering, Chalmers University of Technology, and Rosemary Brown at the Division of Chemical Physics, Department of Physics, Chalmers University of Technology, for manufacturing the PdAu thin film samples for us, as well as the Knut and Alice Wallenberg Foundation for funding through the project 'Atomistic design of new catalysts', project number KAW 2015.0058.

Appendix

Description of the analysis method

For the analysis of the degree of oxidation and preferential ordering, we use an azimuthal integration as shown for the $Pd_{15}Au_{05}$ sample in Fig. 10. The green solid and yellow dashed boxes indicate the areas that are used for the analysis, as shown in Fig. 11A–D and E–H for powder diffraction rings of the oxide 101 and metal 111, respectively.

To estimate the degree of oxidation, the data is projected on the Q axis and integrated by a Gaussian peak on a linear background, as shown in Fig. 11A and E. The intensity of the metal peak is reduced to compensate for the stronger scattering of Au, as compared to Pd. Further, we neglect the small change in atomic form factor over the small Q range and the density difference between metal and PdO. For the analysed reflections, all Pd atoms scatter in phase, while the scattering from the O atoms in the PdO cancels. Hence we get the degree of oxidation, in the probed part of the film, by a direct comparison of the intensities.

To estimate the degree of preferential ordering, the data in Fig. 11B and F instead show a projection on the azimuthal angle. The preferential ordering gives rise to concentrated peaks on the background of the less ordered material. Different orientations appear at different angles, as indicated. The are two peaks corresponding to the [301] orientation, [301] and [301]′, and we use the [301] peak for the further analysis.

The data are fitted by Gaussian peaks on a background described by a second order polynomial plus two or one broad Gaussian peaks, for the oxide and metal, respectively. The fits in Fig. 11B and F show the total fit in red and the background in yellow. C and G show the data after background subtraction, and the fitted peaks.

We define the total degree of preferential ordering as the sum of the area of the peaks divided by the total area found in Fig. 11A and E. The ratio between the different orientations is given by the intensities of the corresponding areas. For this, however, the peak areas first need to be normalised against their multiplicity, which is 1 for the PdO[301] orientation, 2 for PdO[100], PdO[110] and Pd[110] and 3 for Pd[111].

This is by no means a quantitative analysis, but useful for a rough comparison between the different samples.

References

[1] G. Myhre, D. Shindell, F.-M. Bréon, W. Collins, J. Fuglestvedt, J. Huang, D. Koch, J.-F. Lamarque, D. Lee, B. Mendoza, T. Nakajima, A. Robock, G. Stephens, T. Takemura, H. Zhang, Anthropogenic and natural radiative forcing, in: T.F. Stocker, D. Qin, G.-K. Plattner, M. Tignor, S.K. Allen, J. Boschung, A. Nauels, Y. Xia, V. Bex, P.M. Midgle (Eds.), Climate Change 2013: The Physical Science Basis, in: Contribution of Working Group I to the Fifth Assessment Report of the Intergovernmental Panel on Climate Change, Cambridge University Press, Cambridge, United Kingdom and New York, NY, USA, 2013, pp. 659–740, Ch. 8.

[2] I. Chorkendorff, J.W. Niemantsverdriet, Concepts of Modern Catalysis and Kinetics, Wiley-VCH Verlag GmbH & Co. KGaA, 2017.

[3] A. Hellman, A. Resta, N.M. Martin, J. Gustafson, A. Trinchero, P.A. Carlsson, O. Balmes, R. Felici, R. Van Rijn, J.W. Frenken, J.N. Andersen, E. Lundgren, H. Grönbeck, The active phase of palladium during methane oxidation, J. Phys. Chem. Lett. 3 (6) (2012) 678–682, http://dx.doi.org/10.1021/jz300069s.

[4] N.M. Martin, M. Van Den Bossche, A. Hellman, H. Grönbeck, C. Hakanoglu, J. Gustafson, S. Blomberg, N. Johansson, Z. Liu, S. Axnanda, J.F. Weaver, E. Lundgren, Intrinsic ligand effect governing the catalytic activity of Pd oxide thin films, ACS Catal. 4 (10) (2014) 3330–3334, http://dx.doi.org/10.1021/cs5010163.

[5] J.F. Weaver, Surface chemistry of late transition metal oxides, Chem. Rev. 113 (6) (2013) 4164–4215, http://dx.doi.org/10.1021/cr300323w.

[6] J. Rogal, K. Reuter, M. Scheffler, Thermodynamic stability of PdO surfaces, Phys. Rev. B - Condensed Matter Mater. Phys. 69 (7) (2004) 1–8, http://dx.doi.org/10.1103/PhysRevB.69.075421, arXiv:0310235.

[7] F. Gao, D.W. Goodman, Pd–Au bimetallic catalysts: Understanding alloy effects from planar models and (supported) nanoparticles, Chem. Soc. Rev. 41 (2012) 8009–8020, http://dx.doi.org/10.1039/c2cs35160a.

[8] M.D. Strømsheim, J. Knudsen, M.H. Farstad, L. Sørvik, X. Guo, H.J. Venvik, A. Borg, Near ambient pressure XPS investigation of CO oxidation over Pd3Au(100), Top. Catalysis 60 (17–18) (2017) 1439–1448, http://dx.doi.org/10.1007/s11244-017-0831-z.

[9] L. Hilaire, P. Légaré, Y. Holl, G. Maire, Interaction of oxygen and hydrogen with Pd-Au alloys: An AES and XPS study, Surf. Sci. 103 (1) (1981) 125–140, http://dx.doi.org/10.1016/0039-6028(81)90103-5.

[10] W. Drube, M. Bieler, W.A. Caliebe, H. Schulte-Schrepping, J. Spengler, M. Tischer, R. Wanzenberg, The PETRA III extension, in: AIP Conference Proceedings, 2016, http://dx.doi.org/10.1063/1.4952814.

[11] G. Ashiotis, A. Deschildre, Z. Nawaz, J.P. Wright, D. Karkoulis, F.E. Picca, J. Kieffer, The fast Azimuthal integration Python library: PyFAI, J. Appl. Crystallogr. 48 (2015) 510–519, http://dx.doi.org/10.1107/S1600576715004306.

[12] G.S. Harlow, S. Pfaff, G. Abbondanza, Z. Hegedüs, U. Lienert, E. Lundgren, HAT: A high-energy surface X-ray diffraction analysis toolkit, J. Appl. Cryst 56 (2023) 312–321, http://dx.doi.org/10.1107/S1600576723000092.

[13] H. Okamoto, T.B. Massalski, The Au-Pd (Gold-Palladium) system, Bull. Alloy Phase Diagr. 6 (1985) 229–235, http://dx.doi.org/10.1007/BF02880404.

[14] E. Lundgren, G. Kresse, C. Klein, M. Borg, J.N. Andersen, M. De Santis, Y. Gauthier, C. Konvicka, M. Schmid, P. Varga, Two-dimensional oxide on Pd(111), Phys. Rev. Lett. 88 (2002) 246103, http://dx.doi.org/10.1103/PhysRevLett.88.246103.

[15] M. Nicholas, The strength of metal/alumina interfaces, J. Mater. Sci. 3 (1968) 571–576.

[16] Z. Li, F. Gao, Y. Wang, F. Calaza, L. Burkholder, W.T. Tysoe, Formation and characterization of au/pd surface alloys on pd(111), Surf. Sci. 601 (8) (2007) 1898–1908, http://dx.doi.org/10.1016/j.susc.2007.02.028.

[17] A.F. Lee, C.J. Baddeley, C. Hardacre, R.M. Ormerod, R.M. Lambert, G. Schmid, H. West, Structural and catalytic properties of novel Au/Pd bimetallic colloid particles: EXAFS, XRD, and acetylene coupling, J. Phys. Chem. 99 (16) (1995) 6096–6102.

[18] V. Mehar, H. Edström, M. Shipilin, U. Hejral, C. Wu, A. Kadiri, S. Albertin, B. Hagman, K. von Allmen, T. Wiegmann, S. Pfaff, J. Drnec, J. Zetterberg, E. Lundgren, L.R. Merte, J. Gustafson, J.F. Weaver, Formation of epitaxial PdO(100) during the oxidation of Pd(100), J. Phys. Chem. Lett. 14 (2023) 8493–8499, http://dx.doi.org/10.1021/acs.jpclett.3c01958.

[19] H.H. Kan, J.F. Weaver, Mechanism of PdO thin film formation during the oxidation of Pd(111), Surf. Sci. 603 (2009) 2671–2682, http://dx.doi.org/10.1016/j.susc.2009.06.023.

[20] N. Kasper, P. Nolte, A. Stierle, Stability of surface and bulk oxides on Pd(111) revisited by in situ X-ray diffraction, J. Phys. Chem. C 116 (2012) 21459–21464, http://dx.doi.org/10.1021/jp307434g.

[21] O. Løvvik, Surface segregation in palladium based alloys from density-functional calculations, Surf. Sci. 583 (1) (2005) 100–106, http://dx.doi.org/10.1016/j.susc.2005.03.028.